Results in Physics 5 (2015) 314–321

Contents lists available at ScienceDirect

Results in Physics

journal homepage: www.journals.elsevier.com/results-in-physics

The novel transparent sputtered p-type CuO thin films and Ag/p-CuO/n-Si Schottky diode applications

A. Tombak [a], M. Benhaliliba [b,*], Y.S. Ocak [c], T. Kiliçoglu [a,c]

[a] Department of Physics, Faculty of Science, Batman University, Batman 72100, Turkey
[b] Department of Material Technology, Physics Faculty, USTO-MB University, BP1505 Oran, Algeria
[c] Dicle University, Education Faculty, Science Department, 21280 Diyarbakir, Turkey

ARTICLE INFO

Article history:
Received 5 September 2015
Accepted 2 November 2015
Available online 6 November 2015

Keywords:
p-Type CuO
DC sputtering
Crystalline structure
Optical properties
HMS measurement
Schottky diode

ABSTRACT

In the current paper, the physical properties and microelectronic parameters of direct current (DC) sputtered p-type CuO film and diode have been investigated. The film of CuO as oxide and p-type semiconductor is grown onto glass and n-Si substrates by reactive DC sputtering at 250 °C. After deposition, a post-annealing procedure is applied at various temperatures in ambient. Through this research, several parameters are determined such structural, optical and electrical magnitudes. The thickness of CuO thin films goes from 122 to 254 nm. A (1 1 1)-oriented cubic crystal structure is revealed by X-ray analysis. The grain size is roughly depending on the post-annealing temperature, it increases with temperature within the 144–285 nm range. The transmittance reaches 80% simultaneously in visible and infrared bands. The optical band gap is varied between 1.99 and 2.52 eV as a result of annealing temperature while the resistivity and the charge carrier mobility decrease with an increase in temperature from 135 to 14 Ω cm and 0.92 to 0.06 cm^2/Vs, respectively. The surface of samples is homogenous, bright dots are visible when temperature reaches the highest value. As a diode, Ag/CuO/n-Si exhibits a non-ideal behavior and the ideality factor is about 3.5. By Norde method, the barrier height and the series resistance are extracted and found to be 0.96 V and 86.6 Ω respectively.

Introduction

In last decades researchers have given more importance to oxides fabrication and characterization such tin (SnO_2), zinc (ZnO), cadmium (CdO) and copper (CuO) oxides [1–4]. It is well known that two routes are suitable to deposit oxide layers, physical and chemical processes. DC sputtering is a physical deposition technique which used the vacuum at high pressure around 10^{-7} Torr as cited in the literature [5]. There are two stable copper oxide phases according to oxygen composition. One is cupric oxide (CuO) which has a monoclinic phase; the other one is cuprous oxide (Cu_2O) and has a cubic phase [6]. CuO owns specific structural properties which are well known in the literature such as a density of 6.31 g/cm^3, a high melting point of 1200 °C, a monoclinic stable phase at 300 K [7]. Further, researchers have been attracted by its electrical and optical parameters like a dielectric constant of 18.1, a refractive index of 1.4 and a direct band gap within the 1.21–1.55 eV range [7] and greater than 2 eV [8]. CuO is a good absorber layer for solar cell production due to its suitable band gap, absorption capabilities and low thermal emittance [9,10]. Furthermore, it constitutes non-toxic and available in abundance elements, so it is an advantage using CuO in device fabrication. Metal–semiconductor (MS) structures have been widely used for applications in electronic industry for many years. These applications are Schottky barrier diodes, field effect transistors, phototransistors, microwave field effect transistors and so on [11,12]. Conduction mechanism in Schottky barrier diodes has been a debate for decades. There have been several methods based on thermionic emission theory about extracting Schottky diode parameters using current–voltage measurement. One of the important methods, Norde [13] has suggested was a function to determine series resistance and barrier height. Cheung and Cheung proposed a new method [14] by using forward bias current–voltage *I–V* characteristics to evaluate series resistance, barrier height and ideality factor, which has a different approach compared to the Norde's method.

In this study, we prepare CuO films onto glass and n type silicon substrates by reactive magnetron sputtering and those films are annealed from 250 °C to 550 °C with 100 °C step in ambient. The structural properties of the films are investigated by X-ray diffraction. Current versus voltage of CuO/n-Si diode in dark and light is

* Corresponding author. Tel.: +213 772211491.
E-mail address: mbenhaliliba@gmail.com (M. Benhaliliba).

http://dx.doi.org/10.1016/j.rinp.2015.11.001
2211-3797/

measured. Throughout this study, we determine the electrical properties of the thin films such as charge concentration, conductivity type, sheet resistance and mobility for future applications. The optical properties are measured using a spectrophotometer in the 200 nm and 2600 nm range.

Experimental procedure

A Cu–O layer is grown by reactive DC sputtering using copper target (99.99% purity, K.J. Lesker) by applying a power of 44 W. Base pressure before deposition is 4×10^{-6} Torr. The glass and n type silicon substrates temperature is kept at 250 °C during the deposition. Ar/O_2 mixture with a ratio of (4:1) is selected as the reactive gas for plasma sputtering. Each soda lime glass (SLG) is loaded to tube furnace and they are annealed from 250 to 550 °C in ambient air for half an hour. The silver front contacts (Ag/CuO/n-Si) are made into 450 °C annealed sample by thermal evaporation in vacuum at 10^{-6} Torr using a mask. A cross section schematic of the Ag/CuO/Si/Au structure is shown in Fig. 1. The crystal structure properties of the deposited CuO film are investigated using X-ray diffraction (XRD) with Cu K_α radiation ($\lambda = 1.54$ Å), with an angle range (2θ) of 20°–60°, Bruker D8 DISCOVER. The optical properties such as transmittance, reflectance and optical band gap from absorption data are determined using a Shimadzu 3600UV-VIS-IR spectrophotometer in the range 200–2600 nm. The electrical properties of the film are studied using Ecopia HMS3000 Hall Effect Measurement System in a van der Pauw configuration. The scanning electron microscopy (SEM) images and the cross section of the thin film are obtained using FEI Quanta 250 FEG. Current versus voltage are measured using the Keithley 2400 source meter and a solar simulator.

Results and discussion

Structural properties

X-ray patterns of as-sputtered CuO layers as a function of post-annealing temperature are shown in Fig. 2. XRD shows that the crystal structure of the films is monoclinic with preferential orientation of (1 1 1) peaking at 36.72°. This orientation is shifted toward higher angle as temperature increases as tabulated below (Table 1). As we can observe the full width at height medium FWHM values, we can conclude that the peaks are so thin in particular for 450 and 550 °C. It is also seen from Table 1, that the CuO phase is the predominant phase in our samples although the Cu_2O phase occurs at a lower temperature. This behavior is in good agreement with those found in the literature. Also, the as-deposited films are found to be Cu_2O, and a following annealing (>250 °C) is required to switch Cu_2O into CuO as Mageshwari reported earlier [8]. When temperature exceeds 250 °C, no typical peaks of impurities such as Cu are detected in the X-ray pattern, indicating that the grown films contain pure CuO only.

The cupric oxide (CuO) and its monoclinic unit cell are defined by angles and lattice parameters as follows $\alpha = \beta = 90° \neq \gamma$, $a \neq b \neq c$ [8]. The spectra confirm the presence of monoclinic crystal structure in majority of samples and a preferred direction along the (1 1 1) plane. It is shown from X-rays analysis that the sputtered CuO films, explored in the 2θ-range of 20–60°, are polycrystalline and exhibit two major orientations. Zhang has found the same configuration of reflections [6]. Positions of reflections, composition of samples and (*hkl*) planes are gathered in the Table 1. The main peak positions are shifted with increasing the post-annealing temperature. The (1 1 1) orientation is improved by the highest post-annealing temperature. The lattice parameters *a*, *b* and *c* are determined from the literature and are found to be $a = 4.68$, $b = 3.42$ and $c = 5.12$ Å and orientation angles are $\beta = 99.54°$and $\alpha = \gamma = 90°$ and the distances Cu–O, O–O and Cu–Cu, are respectively 1.96, 2.62 and 2.90 Å [15], the d-space of a monoclinic system is given by [15];

$$\frac{1}{d_{hkl}} = \sqrt{\frac{h^2}{a^2 \sin^2\beta} + \frac{k^2}{b^2} + \frac{l^2}{c^2 \sin^2\beta} - \frac{2hl\cos\beta}{ac\sin^2\beta}} \quad (1)$$

The film grain size *G* is given by Scherrer formula [3],

$$G = \frac{0.94\lambda}{\beta\cos\theta} \quad (2)$$

where λ is the wavelength of the X-ray used ($Cu_{K\alpha}$, 1.54 Å), β is the full width at half maximum which has a maximum intensity and 2θ denotes the Bragg angle. Grain size according to (1 1 1) and (−1 1 1) varied from 14.4 nm to 28.3 nm, and $a = 4.69$, $b = 3.43$ and $c = 5.13$ Å as listed in Table 1. As reported in prior works, the lattice parameters of CuO unit cell *a*, *b* and *c* increased with the annealing temperature which ranged from 400 to 700 °C. The parameters are respectively $4.688 < a(Å) < 4.719$, $3.427 < b(Å) < 3.432$, $5.132 < c(Å) < 5.136$ and grain size goes from 20 to 27 nm as a result of annealing temperature [16].

Optical parameters

The optical properties such as transmittance and optical band gap from absorption data are determined using a spectrophotometer in the range between 200 nm and 2500 nm as sketched in Fig. 3. In UV band, the sample annealed @ 250 °C exhibits a strong transmittance of 33% compared to the samples heated at high post-annealing temperatures and then sharply decreases as

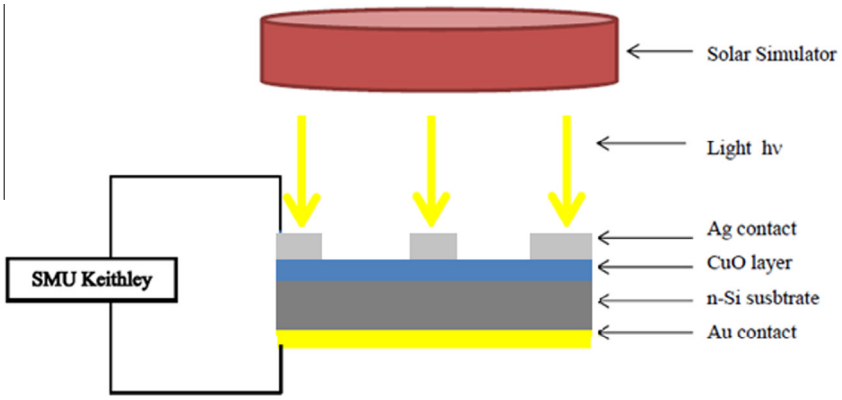

Fig. 1. A cross section schematic of the Ag/p-CuO/n-Si/Au structure.

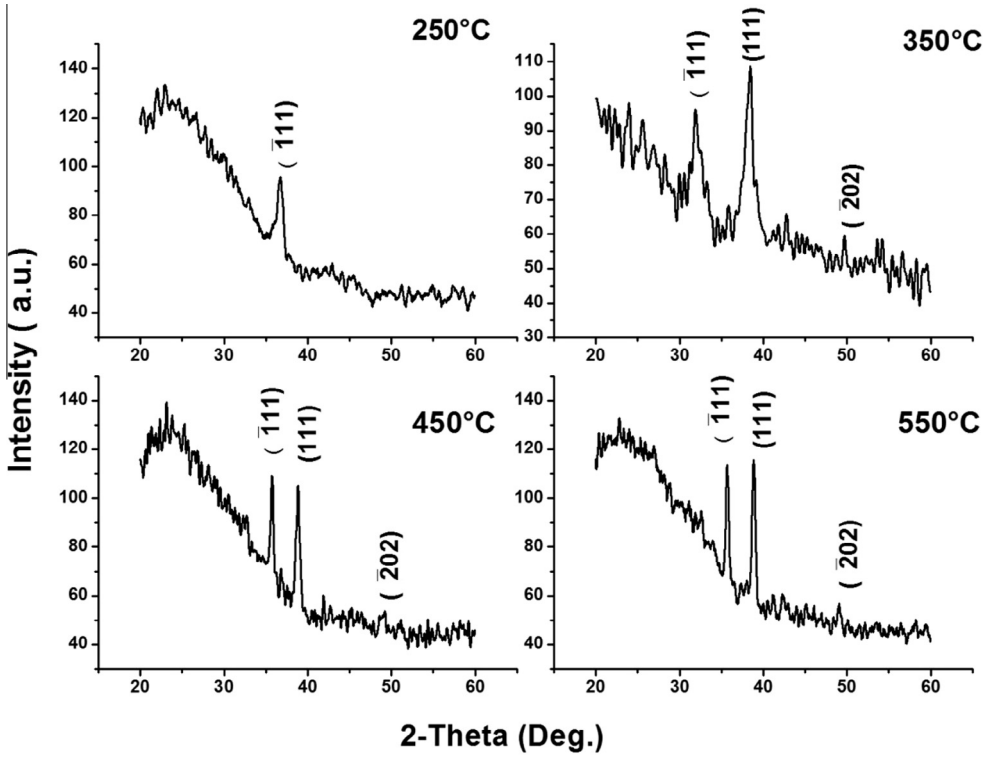

Fig. 2. X-ray pattern of sputtered CuO films post-annealed at various temperatures 250–550 °C. The main peaks are indexed.

Table 1
Bragg angle 2θ, FWHM, grain size, composition and orientation (hkl). JCPDS card #5-661 is mentioned.

	250 °C	350 °C		450 °C		550 °C	
(a)							
2θ (°)	36.72	35.95	39.20	35.74	38.85	35.68	38.84
FWHM (rd)	0.644	0.558	0.457	0.327	0.446	0.449	0.459
Grain size (Å)	144.5	166.4	205	283.5	210.1	206.7	203.9
Composition	Cu_2O	CuO	CuO	CuO	CuO	CuO	CuO
Orientation	(1 1 1)	($\bar{1}$ 1 1)	(1 1 1)	($\bar{1}$ 1 1)	(1 1 1)	($\bar{1}$ 1 1)	(1 1 1)
JCPDS card #5-661	35.58		38.76		38.76		38.76

d-space (Å)	2θ (°)	Peak intensity (%)	*h*	*k*	*l*
(b)					
2.7510	32.55	12	1	1	0
2.5300	35.48	49	0	0	2
2.5230	35.58	100	−1	1	1
2.3230	38.76	96	1	1	1
2.3120	38.95	30	2	0	0
1.8660	48.80	25	−2	0	2

wavelength shifts to visible edge and increases rapidly to reach a peak of 76% in the infrared range @ 826 nm (1.5 eV) (showed by arrow in Fig. 3) and exhibits an edge around 520 nm. The transmittance changes from 74% to 80% in the IR band, this property will give the sputtered CuO special applications in micro-optoelectronic devices. Furthermore, the absorbance increases in the UV region with increasing the annealing temperature. The absorption edge which occurs around 520 nm might be due to the Cu_2O phase which is formed at lower post-annealing temperature and vanishes to higher ones. This latter detail is confirmed by XRD pattern as indicated in Table 1. As seen in Fig. 3, curve of transmittance reaches a high point of 80% in the 450–830 nm wavelength range. The absorption coefficient is expressed as follows [1],

$$\alpha = -\frac{\ln T}{t} \tag{3}$$

where t is the thickness of films ranging between 120 and 255 nm, T is the transmittance and α is the absorption coefficient. The optical band gap is determined by [3];

$$(\alpha h\nu)^2 = (h\nu - E_g) \tag{4}$$

The optical band gap (E_g) of the film is determined by plotting $(\alpha h\nu)^2$ versus photon energy $h\nu$ and extrapolating the straight line portion of this plot to $h\nu$ axis as sketched in Fig. 4. The linear dependence of $(\alpha h\nu)^2$ to $h\nu$ signifies that pure CuO films are direct transition type semiconductors. Consequently, the band gap increases slightly from 1.99 to 2.52 eV as a result of post-annealing

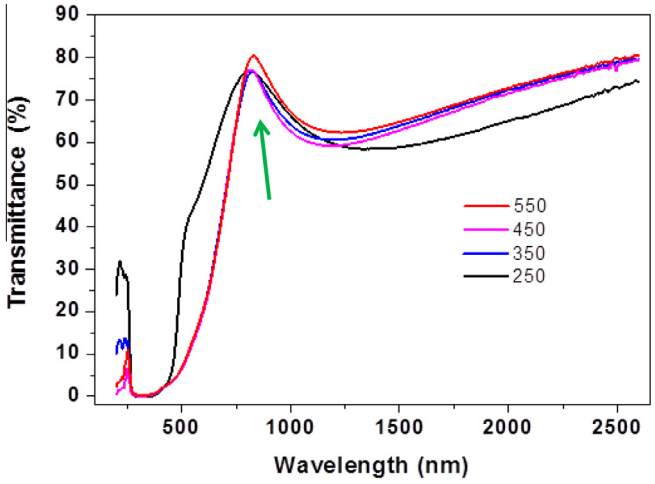

Fig. 3. Transmittance plot versus photon wavelength of sputtered CuO layers annealed at several temperatures. The arrow indicates the peak of 826 nm.

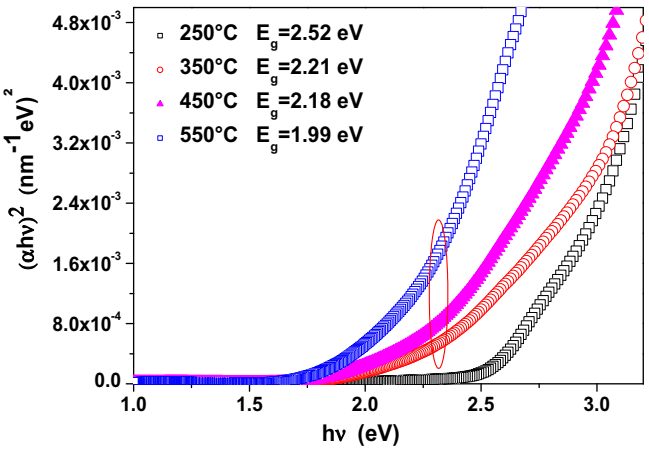

Fig. 4. Plot of $(\alpha h\nu)^2$ as function of photon energy $(h\nu)$ of sputtered CuO layers annealed at several temperatures. The values of E_g are showed in the inset for each post-annealing temperature.

temperature. Our results corroborate with those found in the literature, these oxides are semiconductors having a band gap of 1.2–1.9 eV for CuO and 1.8–2.5 eV for Cu_2O [4,17] while a bulk band gap of Cu_2O ranges within 2.0–2.17 eV as cited by Nunes et al.

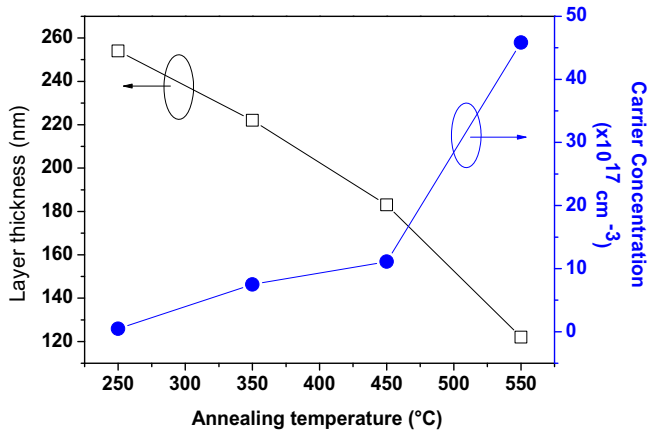

Fig. 6. The layers thickness (left) and the carrier concentration (right) versus post-annealing temperature.

[18]. In the literature, the 2.31–2.48 band gap range for CuO films is also reported [8]. Moreover, Cu_2O phase is a semiconductor having a direct forbidden energy gap of 2.1 eV and the lowest direct allowed optical gap is found to be 2.64 as cited by Musselman et al. [19]. As can be easily seen in Fig. 4, two distinct domains of energy band gap E_g values are revealed, lower one of 2–2.2 eV (assigned by red circle in Fig. 4) and higher one of 2.52 eV. The $(\alpha h\nu)^2$ quantity, in the lower energy domain, increased slowly with increasing the energy since the excitonic transition in this energy gap is parity forbidden and has to be involved with phonons. But around 2.52 eV, a sharp increase in $(\alpha h\nu)^2$ due to the lowest allowed transition is revealed. Similar trends are reported by Briones et al. [20,21].

Electrical measurements

Fig. 5 describes the Hall measurements where the sample is maintained between four gold contacts *M*, *N*, *P* and *Q*. We perform the Hall measurements in order to determine the charge carrier concentration, the resistivity and the mobility as a function of heating temperature. HMS measurements show a decay in carrier concentration with an increased layer thickness versus post-annealing temperature as displayed in Fig. 6 whereas resistivity decreases with layer thickness as shown in the Fig. 7. The charge carrier concentration is found to increase with post-annealing temperature as indicated in Fig. 6, the highest value is around $4.6 \times 10^{18}\ cm^{-3}$ and the mobility ranges from 0.06 to 0.92 cm^2/Vs as listed in Table 2. The hole mobility of CuO, at room

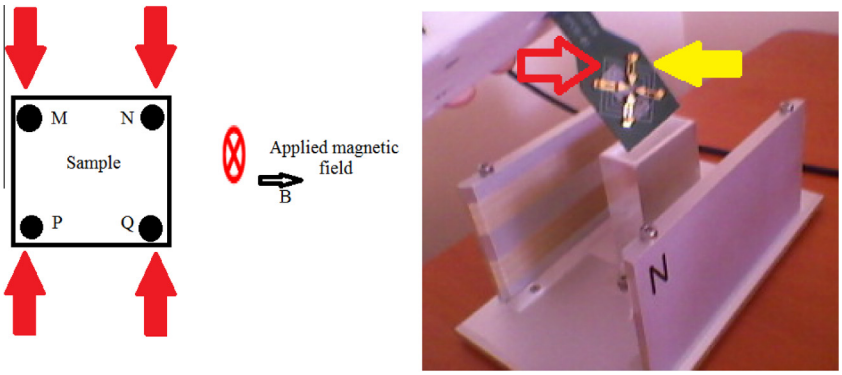

Fig. 5. Hall measurement HMS set up of CuO grown onto glass substrate; the films are retained by four Au probes (red arrow) as signed by yellow arrow (right). As shown at right, the sketch of the samples, the four contacts *M*, *N*, *P*, *Q*, and the magnetic field is applied perpendicularly to the sample. (For interpretation of the references to color in this figure legend, the reader is referred to the web version of this article.)

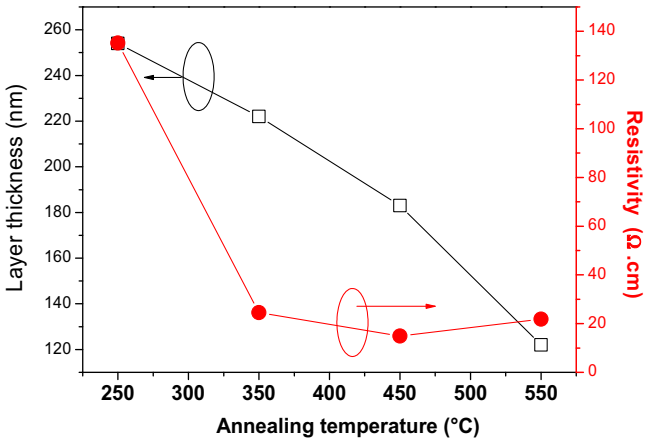

Fig. 7. Layers thickness (left) and resistivity (right) versus post-annealing temperature.

temperature, varying between 0.1 and 10 cm^2/Vs has been previously cited by Amin [7]. The resistivity of the film is expressed as follows [1],

$$\rho = \frac{VS}{Il} \tag{5}$$

V is the measured potential drop across the sample, I is the current through the sample, S is the cross section area through which the current runs and l is the distance separating the voltage leads. The Hall coefficient R_H is given by [1],

$$R_H = \frac{V_H S}{I\mu_0 H l} \tag{6}$$

where V_H is the Hall voltage and $\mu_0 H$ is the magnetic field. Using the HMS measurement, a current of 100 nA runs the sample, the hole concentration is found to be increased with temperature from 0.46 to 45.8×10^{17} cm^{-3}. Sample 4 showed the highest bulk concentration and the lowest mobility of charge carrier by 6×10^{-2} of that of sample 1 as gathered in Table 2. The conductivity type is determined via HMS measurement, as shown in Table 2, the CuO films exhibit a p-type conductivity. Higher bulk concentration around 10^{19} cm^{-3} and lower mobility values of 10^{-5} cm^2/Vs of CuO films, produced by sol–gel route, have been mentioned and the films are resistive $\sim 10^6$ Ω cm [6]. Indeed, the impurities and the oxygen centers originate from the resistivity increase. The increase in post-annealing reduces the amount of the oxygen cations then the resistivity of film becomes minor as indicated in Table 2. Moreover, based on X-rays pattern, an increase in resistance may be due to an increase in the disordered character of the film, a lattice strain and crystalline distortions may also affect the charge transport and then induces an increase in the film resistivity.

The surface morphology investigation

At room temperature and high vacuum, the morphology observation of CuO onto the glass substrate is provided by a scanning electron microscope as shown in Fig. 8. The SEM images are taken at high voltage of 10 kV and at magnification of ×7000–8000. The surface of samples is homogenous, bright dots are visible when temperature reaches highest value of 550 °C and the average of grain size is estimated at 0.2 μm knowing that the micrograph is analyzed with a scale of 10 μm as indicated in bottom right of the SEM picture. It seems that surface showed a whole occurrence which confirms a micro/nano sized particle formation in the films as temperature increases. The CuO synthesized nanostructures have been cited by Zhang [6].

The investigation of the Ag/p-CuO/n-Si heterojunction

Based on the best crystalline structure, the higher transmittance, the lower band gap and the best surface morphology, the sample heated at 550 °C is selected to fabricate the device. The fabrication and electrical characterization of Ag/p-CuO/n-Si inorganic diode have been investigated. Based on the electrical measurement of current versus bias voltage in dark conditions we extract the parameters such as barrier height, ideality factor, saturation current, series resistance and rectifying factor. Fig. 9 shows the semi log I–V characteristics of the Ag/p-CuO/n-Si heterojunction in the dark and illuminated. In light condition, the 150 W corresponds to 100 mW/cm^2 (1.5 AM). As can be seen from the plot that illuminated reverse current is larger than that of under dark. This indicates that under illumination electron–hole pairs are produced in p-CuO/n-Si junction generating then photocurrent. The open circuit voltage (V_{oc}) and the short circuit current (I_{sc}) of the as fabricated heterojunction are found to be 290 mV and 5.5×10^{-4} A, respectively. V_{oc} and I_{sc} values are low causing a degradation of the conversion efficiency. This fact is attributed to the series resistance [22]. As an approximation method, the geometrical construction could determine the maximum power point I_m, V_m, open circuit voltage and short circuit current are displayed in Fig. 9 (inset).

At relatively low forward bias voltages, the current increases exponentially. It can be concluded from the graph that the diode shows rectification behavior with a rectification ratio of 8076 at ±2 V. Therefore, the current can be expressed in terms of voltage and temperature as follows [23],

$$I = I_0\left[\exp\left(\frac{qV}{nkT}\right) - 1\right] \tag{7}$$

where V is the applied voltage, n is the ideality factor is a quantity how the diode closes the ideal behavior, k is the Boltzmann constant, q is elementary charge, T is temperature of measurement and I_0 is reverse saturation current. I_0 can be obtained from the extrapolation of the linear portion of semi-log I–V and is given by,

$$I_0 = AA^*T^2 \exp\left(-\frac{q\phi_{B0}}{kT}\right) \tag{8}$$

where A is the effective diode area (0.0176 cm^2), A^* is the Richardson constant of n-Si (112 A/cm^2 K^2) [23] and ϕ_{B0} the zero bias barrier height of the diode. The obtained I_0 value is 2.3×10^{-8} A. Ideality factor can be extracted from the slope of the linear portion of the ln I–V plot. The calculated ϕ_{B0} and n values are found to be

Table 2
Annealing temperature, film thickness, carrier concentration, resistivity, mobility, conductivity type and conductivity.

Sample	Annealing Temperature (°C)	Film thickness (nm)	Carrier Concentration ($\times 10^{17}$ cm^{-3})	Resistivity (Ω cm)	Mobility (cm^2/Vs)	Conductivity type	Conductivity (10^{-3} Ω cm)$^{-1}$
1	250	254	0.46	135.2	0.92	*p*	7.39
2	350	222	7.48	24.56	0.34	*p*	40.7
3	450	183	11.10	14.91	0.38	*p*	67.1
4	550	122	45.83	21.81	0.06	*p*	45.8

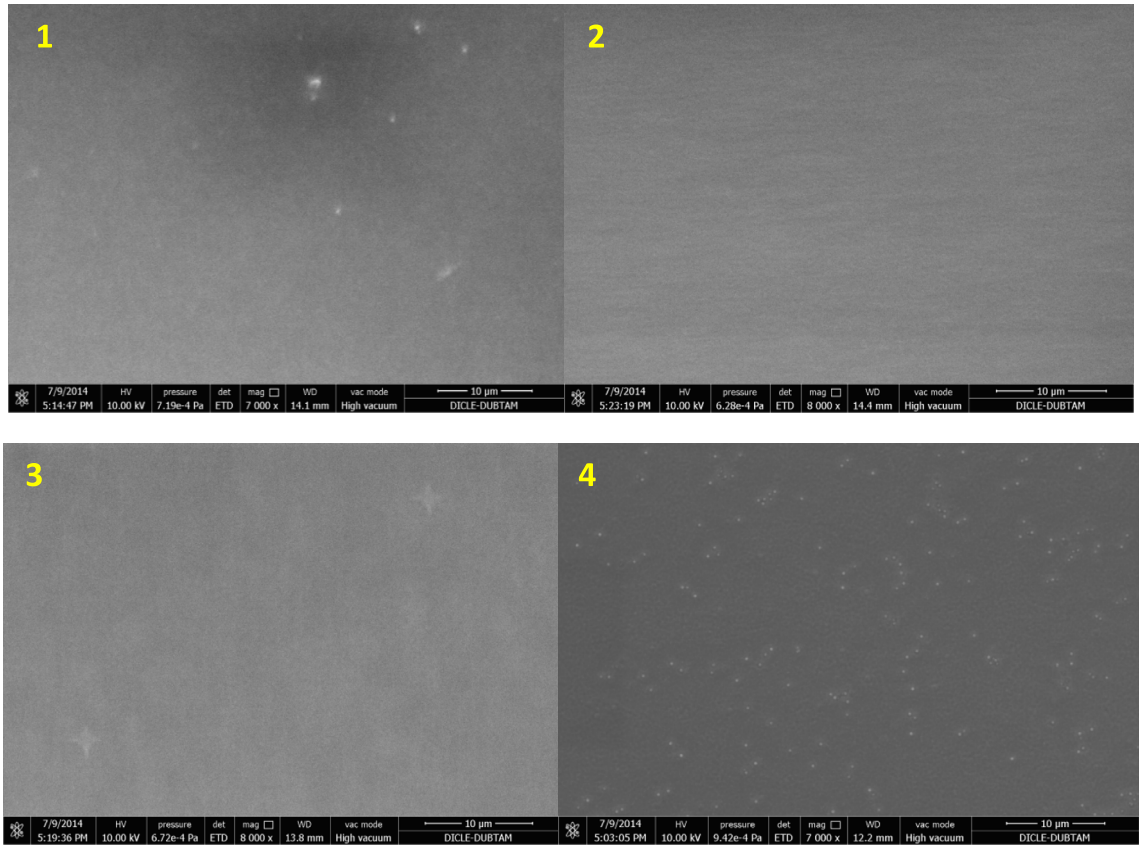

Fig. 8. SEM pictures of sputtered CuO layers at various annealing temperatures (1) 250, (2) 350, (3) 450 and (4) 550 °C.

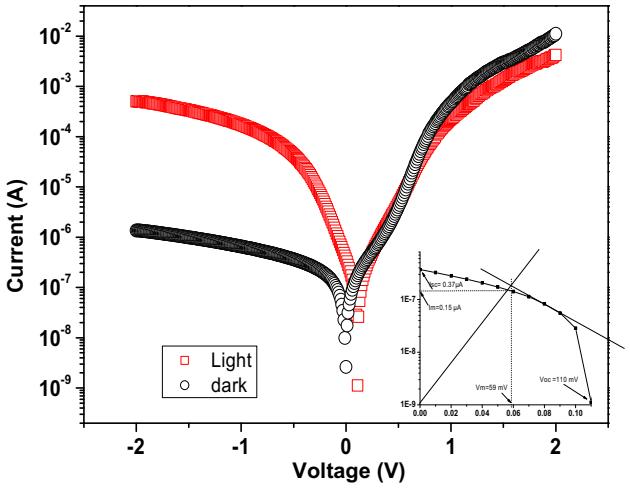

Fig. 9. Plot of current versus voltage (semilog scale) in dark and illumination conditions of Ag/p-CuO/n-Si heterojunction. The geometrical construction of the maximum power point, open circuit voltage and short circuit current are displayed (inset).

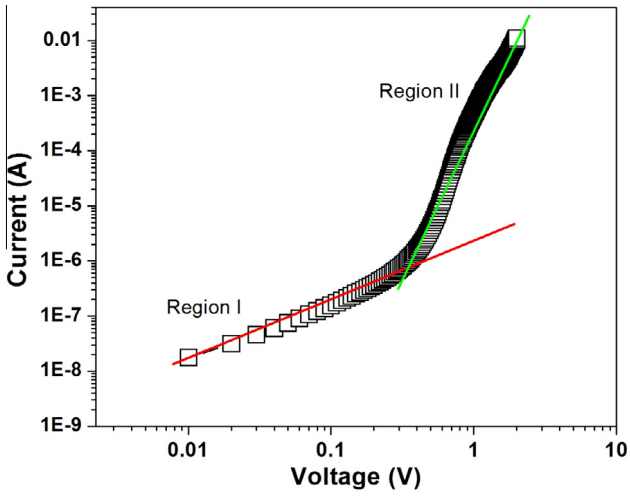

Fig. 10. Log *I–V* plot of Ag/p-CuO/n-Si Schottky diode. The solid lines indicate the regions I and II.

0.75 eV and 3.51, respectively. Several n values are reported in the literature for metal/metal oxide/Si heterostructure for example; Yakuphanoglu et al. reported 14.22 [24] for Al/ZnO/p-Si diode and 5.41 [25] for Al/n-CdO/p-Si heterojunction diode, but Karataş reported 7.20 [26] and Tsiarapas 3.10 [27] for Pd/ZnO/n-Si. High ideality factor, very much greater than unity, may be attributed to many causes like the voltage drop across the CuO layer, the interface states located between CuO layer and Si interface [28,29], the native oxide layer, the series resistance (R_S) suggests that the diode has a metal–insulator–semiconductor (MIS) structure and the presence of a wide distribution of low-Schottky barrier patches is caused by laterally inhomogeneous barrier[30]. To clarify the conduction mechanism of the Ag/p-CuO/n-Si heterojunction under high voltages, logarithmic *I–V* characteristic is analyzed. As observed in Fig. 10, the log *I–V* plots present two distinct current regions. Current obeys the power law of $I \approx \kappa V^m$ [31] where κ is a constant and m is the constant that describes the dominant conduction mechanism of the diode, m equals to 0.99 for the region *I* indicating the current obeys the ohmic regime. In region II obtained m value is 7.25 suggesting a space charge limited current (SCLC) mechanism

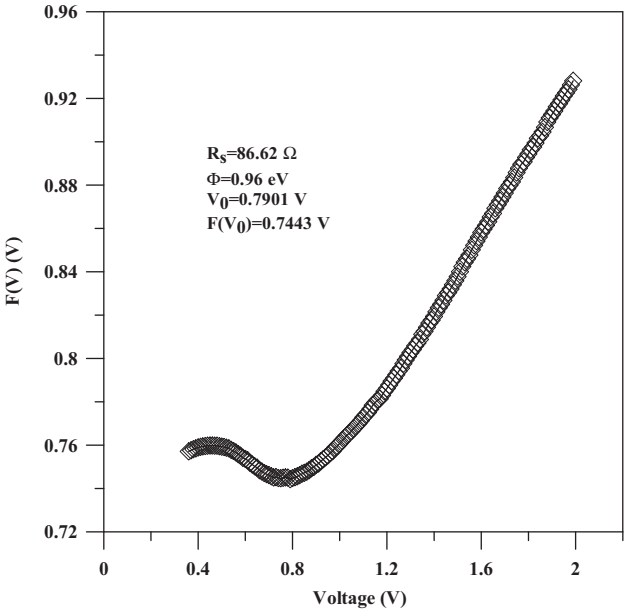

Fig. 11. The variation of the Norde function $F(V)$ versus voltage (V) of Ag/p-CuO/n-Si structure. The value of R_s, Φ, V_0 and $F(V_0)$ are indicated in inset.

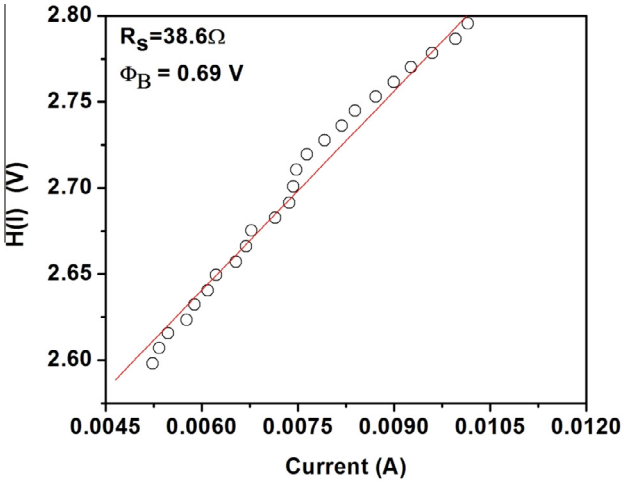

Fig. 12. Sketch of $H(I)$ versus current of Ag/p-CuO/n-Si Schottky diode fabricated by DC sputtering process. The extracted values of series resistance and barrier height are displayed in the inset.

with an exponential distribution of traps in the band gap of the CuO layer [32].

The barrier height and the series resistance of the MIS structure are found by using the method proposed by Norde [13]. The Norde functions are written as follows;

$$F(V) = \frac{V}{\gamma} - \frac{1}{\beta}\left(\frac{I(V)}{AA^{*}T^{2}}\right) \tag{9}$$

where $I(V)$ is the current obtained from I to V data, γ is the first integer greater than n and β is described as q/kT. After determining the minimum value of F versus V plot as shown in Fig. 11, the barrier height can be extracted from the given equation [33],

$$\phi_b = F(V_0) + \frac{V_0}{\gamma} - \frac{1}{\beta} \tag{10}$$

where $F(V_0)$ is the minimum $F(V)$ value of F versus V graph and V_0 is the corresponding voltage value. The series resistance (R_S) of the contact can be defined through the relation [33],

$$R_S = \frac{kT(\gamma - n)}{qI_{\min}} \tag{11}$$

where $I_{\min}$ is the corresponding current value to V_0. Fig. 11 shows the $F(V)$–V graph of the Ag/p-CuO/n-Si diode. The values of ϕ_B and R_S are calculated as 0.85 eV and 80.55 Ω from Eq. (10) to Eq. (11), respectively. The calculated barrier height using Norde functions is higher than that obtained from semi log I–V plot. The difference can be attributed to the nature of these two methods. According to $F(V)$ plot, the series resistance is 86.62 Ω, barrier height is found to be 0.96 V, V_0 is 0.79 V and $F(V_0)$ is 0.74 V. The derivative of voltage $dV/d\ln(I)$ is expressed as follows [34],

$$\frac{dV}{d\ln I} = R_s I + n\left(\frac{kT}{q}\right) \tag{12}$$

when the resistance effect dominates, the two parameters ϕ_{B0} and R_S are determined from the function $H(I)$ [34,35];

$$H(I) = V - \left(\frac{nkT}{q}\right)\ln\left(\frac{I}{AA^{*}T^{2}}\right) \tag{13}$$

However, the function $H(I)$ depending on ϕ_B and R_S, as shown in Fig. 12, can be expressed as follows,

$$H(I) = n\phi_B + R_s I \tag{14}$$

where T is temperature of ambient fixed at 300 K. In the large current region the obtained values of R_S and ϕ_B are 38.6 Ω and 0.69 V. The obtained values are close to that obtained by F–V plots, the two methods are suitable and close to each others.

Conclusion

The DC sputtered p-type CuO thin films and Ag/CuO/n-Si Schottky diode have been studied. The as-grown CuO film onto glass substrate is produced by sputtering. A (1 1 1)-oriented monoclinic crystalline structure is confirmed by XRD analysis. According to (1 1 1) orientation, the lattice parameters are found to be 4.69 Å × 3.40 Å × 5.15 Å and the grain size varied within the range of 140–285 Å as a result of post-annealing temperature. The predominant phase is the cupric oxide which increases crystallinity as annealing temperature increases. The films revealed a high transparency, around 80%, in both Vis and IR bands and optical band gap decreases from 2.52 to 1.99 eV when temperature increases. At high temperature of 550 °C, the bulk concentration, the resistivity and mobility are 46×10^{17} cm^{-3}, 22 Ω cm and 0.06 cm^2/Vs. SEM observation revealed a homogenous surface of films. The extracted electronic parameters are deduced from I–V characteristics and are: $n = 3.5$, $V_{oc} = 0.290$ V, $I_{sc} = 5.5 \times 10^{-4}$ A, the obtained I_0 value is 2.3×10^{-8} A. the non-ideal behavior of as-fabricated diode is confirmed and caused by the series resistance (R_s) occurrence. By Norde method R_s is 86.6 Ω and barrier height is around 0.96 V. Our device based on CuO can be used as a good absorber layer for solar cell.

Acknowledgements

This work is a part of CNEPRU project N^{er} B0L002UN 310220130011 supported by Oran University of Sciences and Technology and MESRS www.mesrs.dz. It is also included in the PNR project under contract number 8/U311/R77, supported by "agen cethématique de rechercheen science et technologie" (ATRST) http://www.atrst.dz/, and National Administration of Scientific Research http://www.dgrsdt.dz. The second author is grateful for

the assistance of virtual library of SNDL https://www.sndl.cerist.dz. We would like to acknowledge the assistance of DUBTAM center head, Dicle University – Diyarbakir Turkey.

References

[1] Benouis C, Benhaliliba M, Mouffak Z, Avila-Garcia A, Tiburcio-Silver A, Lopez MO, Trujillo RR, Ocak Y. The low resistive and transparent Al-doped SnO_2 films: p-type conductivity, nanostructures and photoluminescence. J Alloys Compd 2014;603:213–23.
[2] Benhaliliba M, Benouis C, Mouffak Z, Ocak Y, Tiburcio-Silver A, Aida M, Garcia A, Tavira A, Juarez AS. Preparation and characterization of nanostructures of in-doped ZnO films deposited by chemically spray pyrolysis: effect of substrate temperatures. Superlattices Microst 2013;63:228–39.
[3] Benhaliliba M, Benouis C, Tiburcio-Silver A, Yakuphanoglu F, Avila-Garcia A, Tavira A, Trujillo R, Mouffak Z. Luminescence and physical properties of copper doped CdO derived nanostructures. J Lumin 2012;132:2653–8.
[4] Itoh T, Maki K. Preferentially oriented thin-film growth of CuO (1 1 1) and Cu_2O (0 0 1) on MgO (0 0 1) substrate by reactive DC-magnetron sputtering. Vacuum 2007;81:904–10.
[5] Ocak YS. Electrical characterization of DC sputtered ZnO/p-Si heterojunction. J Alloys Compd 2012;513:130–4.
[6] Zhang Q, Zhang K, Xu D, Yang G, Huang H, Nie F, Liu C, Yang S. CuO nanostructures: synthesis, characterization, growth mechanisms, fundamental properties, and applications. Prog Mater Sci 2014;60:208–337.
[7] Amin G, ZnO and CuO nanostructures: low temperature growth, characterization, their optoelectronic and sensing applications [Dissertation No. 1441]. Linköping Studies in Science and Technology.
[8] Mageshwari K, Sathyamoorthy R. Physical properties of nanocrystalline CuO thin films prepared by the SILAR method. Mater Sci Semicond Process 2013;16:337–43.
[9] Ray SC. Preparation of copper oxide thin film by the sol–gel-like dip technique and study of their structural and optical properties. Sol Energy Mater Sol Cells 2001;68:307–12.
[10] Maruyama T. Copper oxide thin films prepared by chemical vapor deposition from copper dipivaloylmethanate. Sol Energy Mater Sol Cells 1998;56:85–92.
[11] Sun J, Zheng XJ, Li W. A model for the electrical characteristics of metal–ferroelectric–insulator–semiconductor field-effect transistor. Curr Appl Phys 2012;12:760–4.
[12] Vexler MI, Illarionov YY, Suturin SM, Fedorov VV, Sokolov NS. Au/CaF2/nSi (1 1 1) tunnel emitter phototransistor. Solid State Electron 2011;63:19–21.
[13] Norde H. A modified forward *I–V* plot for Schottky diodes with high series resistance. J Appl Phys 1979;50:5052–3.
[14] Cheung SK, Cheung NW. Extraction of Schottky diode parameters from forward current–voltage characteristics. Appl Phys Lett 1986;49:85–7.
[15] Meyer B, Polity A, Reppin D, Becker M, Hering P, Klar P, Sander T, Reindl C, Benz J, Eickhoff M. Binary copper oxide semiconductors: from materials towards devices. Phys Status Solidi B 2012;249:1487–509.
[16] Azam A, Ahmed AS, Oves M, Khan MS, Habib SS, Memic A. Antimicrobial activity of metal oxide nanoparticles against Gram-positive and Gram-negative bacteria: a comparative study. Int J Nanomed 2012;7:6003.
[17] Abaker M, Umar A, Baskoutas S, Kim S, Hwang S. Structural and optical properties of CuO layered hexagonal discs synthesized by a low-temperature hydrothermal process. J Phys D Appl Phys 2011;44:155405.
[18] Nunes D, Santos L, Duarte P, Pimentel A, Pinto JV, Barquinha P, Carvalho PA, Fortunato E, Martins R. Room temperature synthesis of Cu_2O nanospheres: optical properties and thermal behavior. Microsc Microanal 2015;21:108–19.
[19] Musselman KP, Wisnet A, Iza DC, Hesse HC, Scheu C, MacManus-Driscoll JL, Schmidt-Mende L. Strong efficiency improvements in ultra-low-cost inorganic nanowire solar cells. Adv Mater 2010;22:E254.
[20] Caballero-Briones F, Palacios-Padrós A, Calzadilla O, Fausto S. Evidence and analysis of parallel growth mechanisms in Cu_2O films prepared by Cu anodization. Electrochimica Acta 2010;55:4353–8.
[21] Caballero-Briones F, Palacios-Padrós A, Calzadilla O, Moreira I de PR, Fausto S. Disruption of the chemical environment and electronic structure in p-type Cu_2O films by alkaline doping. J Phys Chem C 2012;116(25):13524–35. http://dx.doi.org/10.1021/jp3023937.
[22] Soga T, Kokubu T, Hayashi Y, Jimbo T. Effect of rf power on the photovoltaic properties of boron-doped amorphous carbon/n-type silicon junction fabricated by plasma enhanced chemical vapor deposition. Thin Solid Films 2005;482:86–9.
[23] Sze SM, Ng KK. Physics of semiconductor devices. 3rd ed. New Jersey: John Wiley & Sons; 2007.
[24] Farag AAM, Farooq WA, Yakuphanoglu F. Characterization and performance of Schottky diode based on wide band gap semiconductor ZnO using a low-cost and simplified sol–gel spin coating technique. Microelectro Eng 2011; 88:2894–9.
[25] Yakuphanoglu F, Caglar M, Caglar Y, Ilican S. Electrical characterization of nanocluster n-CdO/p-Si heterojunction diode. J Alloys Compd 2010; 506:188–93.
[26] Karataş Ş, Yakuphanoğlu F. Effects of illumination on electrical parameters of Ag/n-CdO/p-Si diode. Mater Chem Phys 2013;138:72–7.
[27] Tsiarapas C, Girginoudi D, Georgoulas N. Electrical characteristics of Pd Schottky contacts on ZnO films. Mater Sci Semicond Process 2014; 17:199–206.
[28] Tataroglu A, Altindal S. Characterization of current–voltage (*I–V*) and capacitance–voltage–frequency (C–V–f) features of Al/SiO_2/p-Si (MIS) Schottky diodes. Microelectr Eng 2006;83:582–8.
[29] Card HC, Rhoderick EH. Studies of tunnel MOS diodes I. Interface effects in silicon Schottky diodes. J Phys D Appl Phys 1971;4:1589.
[30] Tung RT. Electron transport at metal–semiconductor interfaces: general theory. Phys Rev B 1992;45:13509–23.
[31] Kao KC, Hwang W. Electrical transport in solids. Oxford: Pergamon Press; 1981.
[32] Nastase F, Stamatin I, Nastase C, Mihaiescu D, Moldovan A. Synthesis and characterization of PAni–SiO_2 and PTh–SiO_2 nanocomposites' thin films by plasma polymerization. Prog Solid State Chem 2006;34:191–9.
[33] Güllü Ö, Aydoğan Ş, Türüt A. Fabrication and electrical properties of Al/Safranin T/n-Si/AuSb structure. Semicond Sci Technol 2008;23:075005.
[34] Benhaliliba M, Ocak Y, Benouis C. Effect of metal on characteristics of MPc organic diodes. J Nano Electron Phys 2014;6(4):04009. 3pp.
[35] Kilicoglu T. Effect of an organic compound (methyl red) interfacial layer on the calculation of characteristic parameters of an Al/methyl red/p-Si sandwich Schottky barrier diode. Thin Solid Films 2008;516(6):967–70.